BJR https://doi.org/10.1259/bjr.20210275

Received: 26 February 2021 | Revised: 21 May 2021 | Accepted: 22 June 2021

Cite this article as:
Govaerts CW, van Dijken BRJ, Stormezand GN, van der Weide HL, Wagemakers M, Enting RH, et al. ^{11}C-methyl-L-methionine PET measuring parameters for the diagnosis of tumour progression against radiation-induced changes in brain metastases. *Br J Radiol* 2021; **94**: 20210275.

FULL PAPER

^{11}C-methyl-L-methionine PET measuring parameters for the diagnosis of tumour progression against radiation-induced changes in brain metastases

[1]CHRIS W. GOVAERTS, BSc, [1]BART RJ. VAN DIJKEN, MD, [2]GILLES N. STORMEZAND, MD, [3]HISKE L. VAN DER WEIDE, MD, [4]MICHIEL WAGEMAKERS, MD, PhD, [5]ROELIEN H. ENTING, MD, PhD and [1,6,7]ANOUK VAN DER HOORN, MD, PhD

[1]Department of Radiology (EB44), Medical Imaging Centre (MIC), University Medical Centre Groningen, University of Groningen, Groningen, The Netherlands
[2]Department of Nuclear Medicine and Molecular Imaging, Medical Imaging Centre (MIC), University Medical Centre Groningen, University of Groningen, Groningen, The Netherlands
[3]Department of Radiotherapy, University Medical Centre Groningen, University of Groningen, Groningen, The Netherlands
[4]Department of Neurosurgery, University Medical Centre Groningen, University of Groningen, Groningen, The Netherlands
[5]Department of Neurology, University Medical Centre Groningen, University of Groningen, Groningen, The Netherlands
[6]Brain Tumour Imaging Laboratory, Division of Neurosurgery, Department of Clinical Neuroscience, University of Cambridge, Addenbrooke's Hospital, Cambridge, UK
[7]Department of Radiology, University of Cambridge, Addenbrooke's Hospital, Cambridge, UK

Address correspondence to: Anouk van der Hoorn
E-mail: *a.van.der.hoorn@umcg.nl*

Objectives: Radiation-induced changes (RIC) secondary to focal radiotherapy can imitate tumour progression in brain metastases and make follow-up clinical decision making unreliable. ^{11}C-methyl-L-methionine-PET (MET-PET) is widely used for the diagnosis of RIC in brain metastases, but minimal literature exists regarding the optimum PET measuring parameter to be used. We analysed the diagnostic performance of different MET-PET measuring parameters in distinguishing between RIC and tumour progression in a retrospective cohort of brain metastasis patients.
Methods: 26 patients with 31 metastatic lesions were included on the basis of having undergone a PET scan due to radiological uncertainty of disease progression. The PET images were analysed and methionine uptake quantified using standardised-uptake-values (SUV) and tumour-to-normal tissue (T/N) ratios, generated as SUV_{mean}, SUV_{max}, SUV_{peak}, T/N_{mean}, $T/N_{max\text{-}mean}$ and $T/N_{peak\text{-}mean}$. Metabolic-tumour-volume and total-lesion methionine metabolism were also computed. A definitive diagnosis of either RIC or tumour progression was established by clinicoradiological follow-up of least 4 months subsequent to the investigative PET scan.
Results: All MET-PET parameters except metabolic-tumour-volume showed statistically significant differences between tumour progression and lesions with RIC. Receiver-operating-characteristic curve and area-under the-curve analysis demonstrated the highest value of 0.834 for SUV_{max} with a corresponding optimum threshold of 3.29. This associated with sensitivity, specificity, positive predictive and negative predictive values of 78.57, 70.59%, 74.32 and 75.25% respectively.
Conclusions MET-PET is a useful modality for the diagnosis of RIC in brain metastases. SUV_{max} was the PET parameter with the greatest diagnostic performance.
Advances in knowledge: More robust comparisons between SUV_{max} and SUV_{peak} could enhance follow-up treatment planning.

INTRODUCTION

Brain metastases account for the majority of intracranial neoplasms, affecting approximately 20% of cancer patients throughout the course of disease.[1,2] They occur most commonly, in order of incidence, in lung and breast cancers, followed by melanoma, colorectal cancer and renal-cell carcinoma.[3] A diagnosed brain metastasis is, in many cases, indicative of a poor prognosis. Treatment generally consists of stereotactic radiotherapy (SRT), occasionally following resection and also combined with systemic therapy in selected cases.[4] Response to such treatment is assessed primarily by MRI,[5–7] recommended to be made at regular intervals.

Anatomical MRI sequences, however, are poorly diagnostic for the differentiation between treatment induced changes and progressive disease.[8–10] Radiation-induced changes (RIC) present as increased contrast-enhancement on post-contrast MRI with perilesional oedema. They thus imitate tumour progression (TP). These RIC in some tumour types are termed 'pseudoprogression'.[11–13]

The one-year cumulative incidence of RIC after SRT in brain metastases is estimated to be 13–14%.[14] Being able to accurately differentiate between TP and RIC is an urgent clinical need, as uncertainty about radiation effect might lead to further unnecessary interventions such as reirradiation.

The diagnostic inadequacy of MRI highlights the need for the use of other imaging modalities, of which ^{11}C-methyl-L-methionine (MET)-positron emission tomography (PET) is one of the most widely utilised in both primary brain tumours and cerebral metastases.[15]

Most studies investigating metastases report a high diagnostic accuracy for MET-PET.[16–21] What remains ambiguous in particular however, is a robust comparison of (semi-quantitative) PET measuring parameters so as to identify those which are the most diagnostically reliable. This need for clarity represents a gap in the literature. Our current study addresses this by investigating the accuracy of MET-PET across multiple PET parameters for the diagnosis of TP against RIC in a retrospective cohort of brain metastasis patients.

METHODS AND MATERIALS

Patients

Informed consent was waived by the local institutional review board. We retrospectively extracted all patients during the period from 2009 to 2015 who had received a MET-PET post-radiotherapy for an intra-axial intracranial metastasis at our hospital in Groningen, the Netherlands. Our selection of patients did not exceed 2015 because our institution has since phased out MET-PET in the context of the differential diagnosis of TP/RIC in favour of perfusion-MRI. Other inclusion criteria were age above 18 years and pathological evidence of primary disease. In all cases, MET-PET was performed because of an enlarging, enhancing lesion at the treatment location on T_1/T_2-MRI (contrast-enhanced) bringing about the diagnostic dilemma of radiological progression being due to either TP or RIC. The MRI diagnosis was inconclusive in all cases in that neither TP or RIC could be definitively ruled out.

41 patients were found. 15 of these patients, however, were excluded for the following reasons: the clinical/radiological follow-up information was deemed inadequate to determine a definitive diagnosis ($N = 2$) and the PET scans were inaccessible ($N = 13$). 26 patients with 31 lesions were therefore included.

PET protocol

Imaging was performed in accordance with the 2006 European Association of Nuclear Medicine procedure guidelines for brain tumour imaging using labelled amino acid analogues.[22] All patients underwent a period of fasting and were then administered intravenous ^{11}C-MET (205 (199-213) MBq (median and interquartile range (IQR) Q1-Q3)). Static imaging was performed 20 minutes after ^{11}C-MET administration in one bed position of five minutes using one of two scanners, a 64-slice Biograph^{TM} mCT with 2-mm spatial resolution (Siemens/CTI, Knoxville, TN, USA) ($N = 15$ lesions) or an ECAT Exact HR+ ($N = 16$ lesions) (Siemens/CTI). No summed frames were used. For the lesions analysed with the Biograph^{TM} mCT scanner, images were reconstructed using Truex + TOF with three iterations and 21 subsets in a 400 × 400 matrix size (zoom 1.0) and a 2-mm Gaussian filter. For the lesions analysed with the PET-HR+ camera, images were reconstructed using OSEM with three iterations and 24 subsets and a 5-mm Gaussian filter.

Imaging analysis

The PET images were analysed with Syngo.via (Siemens Medical Solutions Inc., Knoxville, TN, USA) with blinding to the clinical follow-up data. The images were interpreted alongside the most recent MRI, preferably contrast-enhanced T1W images, prior to the date of the PET scan. This provided an anatomical reference for accurate localisation of the tumour. The volume-of-interest (VOI) tool was used to semi-automatically delineate the VOIs. First, a sphere large enough to include all visual uptake at the lesion site was drawn manually. Then, the VOI was computed algorithmically to include all voxels that demonstrated a tracer uptake higher than a pre-set threshold (40% of SUV_{max}). The 40% of SUV_{max} threshold for tumour delineation is a standard value used in our department and leads consistently to good tumour definition when compared to visual inspection. The VOI tool was then used to determine the MET activity count normalised to injected dose per kilogram of patient body weight, a measurement unit termed standardised-uptake value (SUV or SUV-bw). The SUV was generated as SUV_{mean} (average SUV over a VOI), SUV_{max} (maximum single voxel SUV within a VOI) and SUV_{peak} (average SUV calculated within a 1 cm^3 VOI, which comprises the maximum voxel value).[21]

A 1 cm^3 control VOI was contralaterally placed in a region of grey matter that mirrored the site of disease. Subsequently, the tumour-to-normal tissue (T/N) ratios were calculated, expressed as T/N_{mean}, $T/N_{max\text{-}mean}$, and $T/N_{peak\text{-}mean}$. The T/N_{mean} was calculated by dividing the SUV_{mean} of the lesion by the SUV_{mean} of the control VOI. The $T/N_{max\text{-}mean}$ was derived in the same way but using SUV_{max} from the lesion and the SUV_{mean} of the control VOI, and the $T/N_{peak\text{-}mean}$ using SUV_{peak} from the lesion and the SUV_{mean} from the control VOI. Also determined were the metabolic-tumour-volume (MTV) (metabolically active volume of the lesion VOI), the total-lesion methionine metabolism (TLMM) (product of MTV and SUV_{mean}[23]) and a bidimensional measurement of the lesion size on T_1 (contrast-enhanced) MRI (maximal tumour diameter and the corresponding largest perpendicular diameter).

Definitive diagnosis

The definitive diagnoses for each lesion were identified as either TP or RIC. All of these diagnoses were established in a multidisciplinary team meeting on the basis of radiological and clinical follow-up. Resection by craniotomy is recommended only when

Figure 1. Imaging of a 53-year-old female (case number 6: Supplementary Material 1) with a right lower-lobe lung adenocarcinoma metastasised to the right frontal-lobe. The lesion was resected and subjected to 10.00 × 3.00 Gy whole brain radiotherapy postoperatively. One year later the lesion showed progression, for which 20.00 Gy was given through SRT. The T1W (contrast-enhanced) MRI (a) was made 12 months after the SRT and depicts contrast-enhancement suspect for progression (white arrow). The MET-PET image (b) was performed one month afterwards and shows slight comparative tracer uptake (SUV_{mean} = 2.29, SUV_{max} = 3.39 and SUV_{peak} = 2.61; black arrow). The T1W (contrast-enhanced) MRI (c), performed five months after the PET scan, depicts tumour shrinkage. This was considered sufficient for a diagnosis of RIC. MET-PET, ^{11}C-methyl-L-methionine PET; RIC, Radiation-induced changes; SRT, Stereotactic radiotherapy; SUV, Standardised-uptake-value.

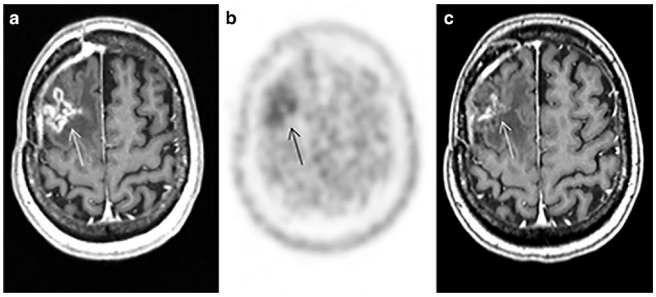

Figure 2. Imaging of a 72-year-old male with a left-lower lobe lung carcinoma (subtype not specified) (case number 26: Supplementary Material 1) metastasised to the right occipital lobe. This patient was treated with 20.00 Gy through SRT. The T1W (contrast-enhanced) MRI (a) was made 1 year and 10 months afterwards, with new enhancement (white arrow). This was followed one month after by a MET-PET scan (b), showing distinct uptake (SUV_{mean} = 3.75, SUV_{max} = 6.18, SUV_{peak} = 4.22; black arrow) suggestive of TP. The T1W (contrast-enhanced) MRI, made 10 days later, highlighted an increase in size both cranially and ventrally (white arrow). Other sequences showed a considerable increase in vasogenic peritumoural oedema. This, along with the deteriorating clinical situation and the follow up reirradiation with SRT (8 × 3.00 Gy), led to the definitive diagnosis of TP. MET-PET, ^{11}C-methyl-L-methionine PET; SRT, Stereotactic radiotherapy; SUV, Standardised-uptake-value; TP, Tumour progression.

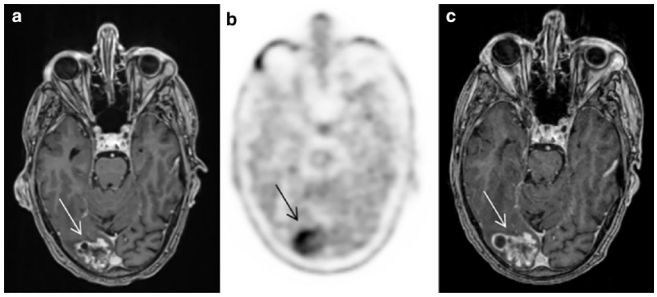

progressive symptoms cannot be suppressed by corticosteroids or radiotherapy alone. Histologic confirmation is, therefore, rarely available and could not be found for any included patients.

A lesion was defined as showing RIC if, for a consecutive period of at least 4 months subsequent to the investigative PET scan, the lesions showed spontaneous reduction or remained stable in size on T_1/T_2 MRI (contrast-enhanced) without any anti tumour treatment, as defined by the Response Assessment in Neuro-Oncology Brain Metastases criteria[7,24] (Figure 1). When possible, the clinical situation was also considered at 6 months, with no further clinical worsening in patients with symptomatic RIC being taken into account.[17,25,26] TP lesions were those that continued to show an increase in size by at least 20% in the longest lesion diameter on MRI for at least 4 months subsequent to the investigative PET scan. Lesions that required reirradiation and/or resection or were confirmed to be the primary cause of the patient's death before 4 months due to a deteriorating clinical situation, with progression of symptoms (such as headache, seizures, and focal neurologic aberrations) and signs of increased intracranial pressure, were also considered as TP (Figure 2).

The follow-up time for lesions with RIC was defined as the period subsequent to the PET scan during which the lesions remained stable or showed consistent reduction in size. For TP lesions, this was defined as the period until death from progressive intracerebral disease, until reirradiation and/or resection due to progressive disease or during which the lesion showed continuous increase in size in successive T_1/T_2 (contrast-enhanced) MRI images.

Statistical analysis

The analyses were performed on a per-lesion basis. All collected PET measuring parameters (SUV_{mean}, SUV_{max}, SUV_{peak}, T/N_{mean}, $T/N_{max\text{-}mean}$, $T/N_{peak\text{-}mean}$, MTV and TLMM) were compared between the TP and RIC diagnostic groups using the Mann–Whitney U non-parametric test after data analysis by way of Shapiro–Wilk and histogram assessment confirmed non-normality. A receiver-operating-characteristic curve was generated and area-under the curve analysis used to determine and compare the diagnostic ability of each parameter in terms of true-positive and false-positive rates. A significance value of $p < 0.05$ was used.

The receiver-operating-characteristic curve was used to define a threshold value by way of Youden's index/J statistic for the diagnosis of TP corresponding to sensitivity and specificity values according to the PET measuring parameter. Positive and negative predictive values were then calculated. The diagnostic threshold was ultimately determined on the basis of maximum positive predictive and negative predictive values, which were considered more clinically relevant diagnostic guides. All analyses with performed with SPSS Statistics v.25.0 (IBM, Armonk, NY) and figures were generated with GraphPad Prism v.9.0.1.151 (GraphPad Software Inc., San Diego, CA).

RESULTS

General characteristics

26 patients with 31 lesions were included. The population consisted of 13 males and 13 females. The median age was 63.5 (53.8–71.0 IQR Q1-Q3) years. The primary sites for each lesion were as follows: lung (N = 17), breast (N = 4), kidney

Figure 3. Box-and-whisker plots for the SUV, TLMM and MTV PET parameters (a) and the T/N PET parameters (b). The panels are split according to measuring parameters and the boxes patterned by definitive diagnosis, as confirmed by clinicoradiological follow-up. The horizontal lines represent the median values for each parameter, the boxes indicate the IQR (Q1–Q3) and the error bars outline the range. MTV: metabolic-tumour-volume; RIC, Radiation-induced changes; SUV, Standardised-uptake-value; TLMM: Total-lesion methionine metabolism; T/N, Tumour-to-normal tissue ratio; TP, Tumour progression.

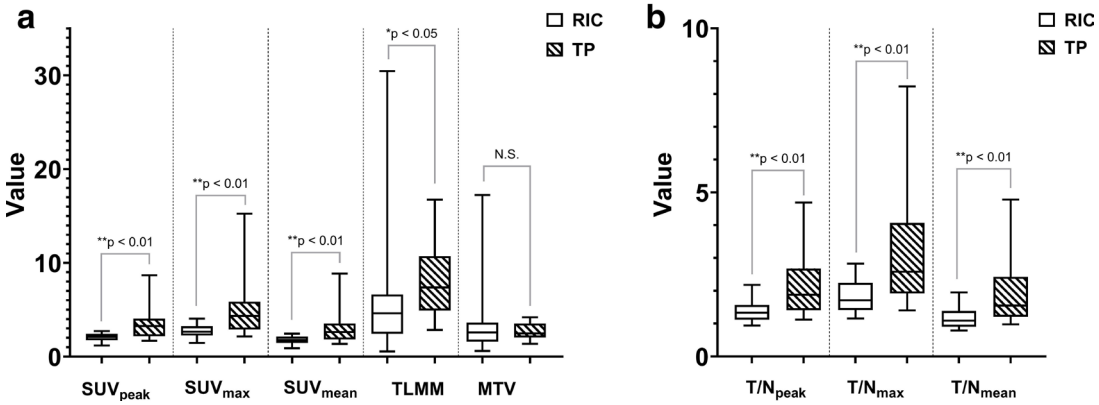

(renal-cell-carcinoma) (N = 1), skin (melanoma) (N = 4), oesophagus (N = 2), colon/rectum (N = 1), connective tissue (fibrosarcoma) (N = 1) and heart (myxoma) (N = 1). The lesions were treated either by SRT only (N = 24), by craniotomy/excision with whole-brain-radiotherapy and SRT (N = 3), by SRT and whole-brain-radiotherapy (N = 1), by craniotomy/excision with only whole-brain-radiotherapy (N = 1) or by craniotomy/excision with only SRT (N = 2) (Supplementary Material 1). The median lesion-specific cumulative radiation dose was 20.00 (20.00–31.30 IQR Q1-Q3) Gy. 14 out of 26 patients were taking dexamethasone at the time of the PET scan. Although the dosage was unknown in five of these patients, the remainder was administered a median daily dosage of 8.0 (3.5–8.00 IQR Q1-Q3) mg. The dosage was not found to be significantly different between the two diagnostic groups using the Mann-Whitney U-test (p = 0.487). The median interval between radiotherapy treatment and the PET scan was 8.8 (5.4–13.0 IQR Q1-Q3) months whilst the median interval between the initial MRI showing an enlarging, enhancing lesion at the treatment location (suggesting either RIC or TP) and the PET scan was 1.07 (0.57–2.43 IQR Q1-Q3) months. The median interval between the most recent pre-PET MRI and the PET scan itself was 0.83 (0.47–1.17 IQR Q1-Q3) months and the median follow-up time subsequent to the PET scan was 3.8 (2.2–5.3 IQR Q1-Q3) months. The median lesion dimensions were 1.92 × 1.56 ((1.10–2.75) × (0.91–2.13) IQR Q1-Q3) cm.

We also performed a basic visual analysis per lesion, outlining the degree of MET uptake and an interpretation of whether this was suggestive of RIC or TP (Supplementary Material 2).

PET measuring parameter comparison

The total number of lesions diagnosed definitively as showing RIC and TP were 14 and 17, respectively. The median and IQR values were calculated for each parameter (Figure 3 and Table 1).

Comparing the parameters by definitive diagnosis with the Mann–Whitney U-test yielded significant differences for all with the exception of MTV (SUV_{mean}, p = 0.004; SUV_{max}, p = 0.002; SUV_{peak}, p = 0.004; T/N_{mean}, p = 0.007; $T/N_{max\text{-}mean}$, p = 0.006; $T/N_{peak\text{-}mean}$, p = 0.008; TLMM, p = 0.039 and MTV, p = 0.781).

A separate analysis was also performed to compare the parameter values according to camera type and definitive diagnosis (Supplementary Material 3). The Mann–Whitney U-test only showed significance for the SUV_{max}, T/N_{mean} and $T/N_{max\text{-}mean}$ parameters between the two camera types within the TP group. No significance was shown for the parameters within the RIC group.

Tests for diagnostic ability

A receiver-operating-characteristic curve was compiled using the PET measuring parameter data and the corresponding

Table 1. MET-PET measuring parameter quantitative comparison

Definitive diagnosis	SUV_{mean} [b]	SUV_{max} [b]	SUV_{peak} [b]	T/N_{mean} [b]	$T/N_{max\text{-}mean}$ [b]	$T/N_{peak\text{-}mean}$ [b]	TLMM[a]	MTV
RIC (N = 14)	1.79 (1.46–2.13)	2.66 (2.26–3.25)	2.11 (1.74–2.44)	1.09 (0.87–1.33)	1.71 (1.41–2.18)	1.33 (1.08–1.49)	4.63 (2.43–6.65)	2.59 (1.61–3.62)
TP (N = 17)	2.63 (1.84–3.53)	4.35 (2.89–5.86)	3.27 (2.17–4.07)	1.55 (1.19–2.23)	2.58 (1.89–3.73)	1.88 (1.41–2.46)	7.37 (4.90–10.72)	2.47 (2.05–3.54)

MTV, Metabolic-tumour-volume; RIC, Radiation-induced changes; SUV, Standardised-uptake value; TLMM, Total-lesion methionine metabolism; T/N, Tumour-to-normal tissue ratio; TP, Tumour progression.
Median and IQR (Q1-Q3) for each MET-PET measuring parameter according to the definitive diagnosis.
[a] p < 0.05 (Mann-Whitney U-test).
[b] p < 0.01 (Mann–Whitney U-test).

Figure 4. Receiver-operating-characteristic curves for the SUV PET parameters (a), the T/N PET parameters (b) and the MTV/TLMM PET parameters (c). The curves indicate the trade-off between true-positive (sensitivity) and false-positive (1-specificity) rates for the differentiation between TP and RIC using each parameter. The perfect diagonal line for each panel is the reference or 'random-guess' line. MTV, Metabolic-tumour-volume; RIC, Radiation-induced changes; SUV, Standardised-uptake-value; T/N, Tumour-to-normal tissue ratio; TLMM, Total-lesion methionine metabolism; TP, Tumour progression.

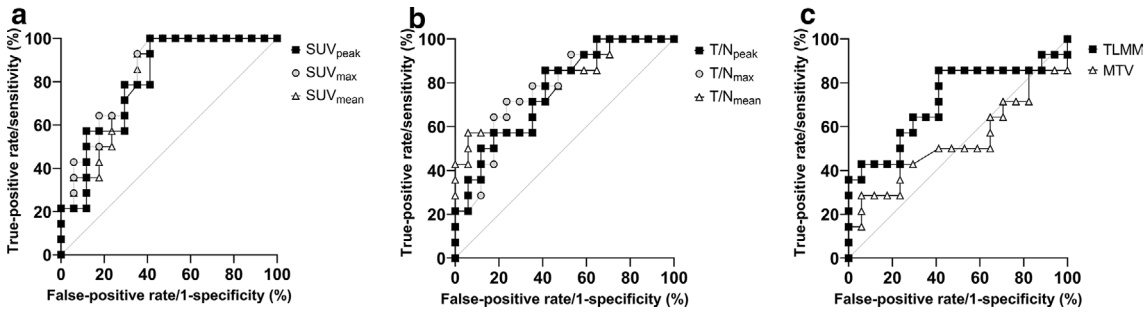

definitive diagnoses (Figure 4). The area under the curve analysis yielded the following results: SUV_{mean} = 0.809 [95% CI (0.656, 0.961)]; SUV_{max} = 0.834 [95% CI (0.693, 0.975)]; SUV_{peak} = 0.807 [95% CI (0.653, 0.961)]; T/N_{mean} = 0.779 [95% CI (0.614, 0.945)]; $T/N_{max\text{-}mean}$ = 0.779 [95% CI (0.617, 0.942)]; $T/N_{peak\text{-}mean}$ = 0.767 [95% CI (0.602, 0.932)]; TLMM = 0.719 [95% CI (0.527, 0.910)] and MTV = 0.529 [95% CI (0.312, 0.747)].

According to Youden's index/J statistic by way of maximising both the positive and negative predictive values, the threshold value for the diagnosis of TP for SUV_{max} was 3.29 (sensitivity: 78.57%, specificity: 70.59%, positive predictive value: 74.32% and negative predictive value: 75.25%). The values for SUV_{mean}, SUV_{peak}, $T/N_{max\text{-}mean}$, T/N_{mean}, $T/N_{peak\text{-}mean}$ and TLMM respectively were 2.00 (sensitivity: 71.43%, specificity: 70.59%, positive predictive value: 74.97% and negative predictive value: 55.70%), 2.45 (sensitivity: 78.57%, specificity: 70.59%, positive predictive value: 74.32% and negative predictive value: 75.25%), 2.03 (sensitivity: 71.43%, specificity: 70.59%, positive predictive value: 72.46% and negative predictive value: 69.52%), 1.33 (sensitivity: 71.43%, specificity: 64.71%, positive predictive value: 68.68% and negative predictive value: 67.65%), 1.40 (sensitivity: 71.43%, specificity: 64.71%, positive predictive value: 70.56% and negative predictive value: 64.32%) and 6.45 (sensitivity: 64.29%, specificity: 64.71%, positive predictive value: 66.37% and negative predictive value: 62.58%).

DISCUSSION

The current study is one of the few to comprehensively compare multiple PET measuring parameters in distinguishing RIC and TP during the follow-up of brain metastases. Furthermore, this is one of the only studies to investigate the diagnostic performance of SUV_{peak}, $T/N_{peak\text{-}mean}$ and TLMM in brain metastasis patients. We have now demonstrated the utility of MET-PET in this context and have shown that SUV_{max} is the most diagnostically reliable parameter in our patient group.

The ability of MET to distinguish between RIC and TP has been widely documented in primary brain tumours.[15–17] This represents the majority of the available literature. The Response Assessment in Neuro-Oncology Brain Metastases criteria consider amino acid PET modalities to be useful in the differentiation between recurrent tumours and post-therapeutic changes following radiotherapy.[7,24] The current study is one of a handful that evaluates the diagnostic performance of MET-PET in brain metastases.[16–21,27] The majority of these, with some exceptions,[16] have focused either on comparisons with other tracers, involve smaller sample sizes, or address the question of diagnostic performance as a secondary outcome measurement. Some studies have also not analysed brain metastases separately from other intracranial tumour types (glioblastoma for example) when determining diagnostic metrics and accuracy thresholds, making the results less relevant to brain metastases specifically. We have addressed these caveats in our investigation and have, in a retrospective setting, provided a more comprehensive clarification of the diagnostic accuracy of the most widely use PET measuring parameters.

Comparing our results of diagnostic performance to analogous studies, we note both an underestimation of sensitivity and specificity and a difference in area-under-the-curve analysis results. Terakawa et al[16], in their study of 56 metastatic lesions, reported the highest area-under-the-curve of 0.780 for T/N_{mean}, with a threshold of 1.41 corresponding to sensitivity, specificity, positive-predictive and negative-predictive values of 79%, 75%, 70 and 83%, respectively. Tsuyuguchi et al[27] in their prospective analysis of 21 metastasis patients found sensitivity and specificity values for T/N_{mean} of 77.8% and 100.0%, respectively. For $SUV_{mean,}$ these values were 77.7% and 75.0%. They determined a threshold value for T/N_{mean} of 1.42. These are both higher thresholds than our 1.33 for T/N_{mean} and associated with consistently better diagnostic performance for most metrics. These differences may be due to these studies' larger sample size. Also notable is that the definitive diagnoses were made according to pathological assessment in both studies, which is the gold standard. The study by Tsuyuguchi et al[27] was also prospective, allowing the control of variables such as camera type, methionine dosage and treatment modality. This being said, our analysis reports higher positive-predictive values when using SUV_{max} at a threshold of 3.29. In theory, the utility of SUV_{max} in brain metastases is due to its reliable detection of small progressive lesions, which are highly prevalent in our cohort. Interestingly, MTV was not predictive. TLMM, on the other hand, appears to be a useful parameter, with an area-under-the-curve value of 0.719.

In a recent study by van Dijken et al[23], greater values for both TLMM and MTV were shown to be significantly associated with a poorer prognosis in glioma patients. Volume on its own may, therefore, be predictive for aggressiveness in confirmed TP cases, but it must be combined with uptake for it to be diagnostic for RIC. Our data show that even large contrast-enhanced lesions on MRI do not necessarily indicate underlying progressive disease.

SUV_{peak} is a noticeably underused measuring parameter in PET-related literature.[28] For intracranial neoplasms, a handful of articles are available utilising SUV_{peak} as a measure of treatment response, but only in other radiotracers such as FDG-PET.[29] We report a promising diagnostic accuracy for MET-PET derived SUV_{peak} according to its area-under-the-curve value of 0.807. SUV_{peak} is interesting because it is generated by measuring the average voxels over a 3D sphere of specific volume, which is focused on the highest uptake portion of a tumour. This way it is not reliant on a single voxel of maximum uptake, as in SUV_{max}.[30] It is thus also theoretically a more flexible parameter and adaptable according to tumour size. This is probably why it seemed successful in our patient group, as it possibly adjusted to the heterogeneity both within tumours and across different tumour types. We suspect that part of the reason SUV_{max} saw greater success in our cohort as compared with SUV_{peak}, was that in larger lesions with considerable heterogeneity, there is a higher probability for voxels with marked SUVs. These likely distorted the diagnostic tests in favour of this parameter, the effects of which are compounded by our relatively small sample size. Given the until now limited study into the dynamics of SUV_{peak} and its utility in treatment follow-up, we stress the need for future evaluation comparing the value of this parameter with SUV_{max}.

Comparing our findings to PET studies using other radiolabelled amino acids showed distinct differences in diagnostic metrics. A study investigating *O*-(2-[^{18}F]fluoroethyl)-L-tyrosine (FET) in 62 brain metastasis patients with 76 lesions showed greater sensitivity and specificity values both for T/N_{max} (sensitivity = 83%; specificity = 85%) and T/N_{mean} (sensitivity = 86%; specificity = 88%).[31] The threshold values for these two parameters were 2.55 and 1.95, respectively. A study investigating L-3,4-dihydroxy-6-^{18}F-fluoro-phenylalanine (FDOPA) in 32 brain metastasis patients with 83 lesions also reported greater diagnostic accuracy for T/N_{max} and T/N_{mean}. These parameters showed sensitivity and specificity values of 81.3% and 72.5% at thresholds of 2.02 and 1.70, respectively.[32] It is difficult to state whether or not the results of these studies imply a greater utility of FET and FDOPA-PET compared to MET-PET. These studies, in addition to this investigation, were performed retrospectively. Whilst of course still valuable, this makes direct comparison difficult. There are other studies investigating MET-PET reporting similarly high diagnostic accuracy measurements to these two examples such that the RANO/PET group does not make concrete statements as to which radiolabelled amino acid is superior.[24] This highlights the need for prospective studies comparing all three analogues using similar protocols in the same patient cohort.

Notable is that our institution has since the end of patient inclusion for this study (2015) phased out MET-PET in favour of perfusion-MRI. The primary reason for this was cost related (maintenance and manning of an on-site cyclotron) and the fact that perfusion-MRI has been found to be sufficiently reliable in the context of the diagnostic dilemma of RIC against TP.

Interestingly, two lesions, cases 2 and 3, which were found in the same NSCLC patient, were notable in that they were ultimately diagnosed as showing TP although displaying very low SUV and T/N values. The PET images showed slight increased MET activity with localisations corresponding to the lesions on the most recent pre-PET MRI. Visually the MET activity would suggest RIC for both lesions, yet they continued to show progression on MRI for several months after follow-up (the uncertainty about the diagnosis led to an additional MET-PET, which showed similar MET activity as previously) to the point that the lesions were reirradiated for symptom relief. This suggests that some lesions might continue to show progression despite minimal corresponding amino acid uptake, stressing the need to always consider clinical presentation and lesion growth on sequential MRI.

Our study has several limitations. Most are inherent to the retrospective design. The first is that the results of the PET scans were known to the treating physicians at the multidisciplinary team meetings. This implies that the scans may have affected clinical decision-making during follow-up, representing a bias. Noteworthy also is that the median follow-up length is less than 4 months in our cohort. This is because of the TP lesions, for which resection and/or radiotherapy was often performed before 4 months to alleviate progressive symptoms. The second limitation is that different PET cameras were used for the lesion analysis. The spatial resolution is greater for the mCT as compared with the HR+, and this has important implications in terms of an underestimation of smaller-volume lesions due to partial volume effects. This is amplified as the spatial resolution of a camera decreases and is most pronounced in the SUV_{max} parameter. The effect minimises with the SUV_{mean} and SUV_{peak} parameters. This is reflected in our results and the large variation in SUV_{max} values in the TP lesions is striking. Systematic underestimation of the SUVs for small volume lesions has led to marked overlap in values for TP and RIC (Figure 3). We consider this to be compounded also by the heterogeneity of the primary lesions. A similar trend of variation is not as noticeable for the lesions with RIC, which is expected as there is less detectable tumour activity in these cases to bring about partial volume effects. It can be further reasoned based on partial volume effects that the HR+ SUV_{max} measurements in smaller lesions in our cohort have been undervalued comparatively to similar-sized lesions captured with the mCT. The explanation outlined above is also partially why we have placed emphasis on the SUV_{peak} parameter results, where partial volume effects play a significantly less important role.

A third limitation is that using the clinical context as follow up could theoretically lead to a misdiagnosis of TP. This is because RIC are frequently observed in the background of clinical deterioration.[26,33] The last drawback is that we could not control the treatment modality in our patients, as this was determined on an individual basis in the clinic.

CONCLUSION

We have demonstrated the utility of several MET-PET measuring parameters and, in particular, of SUV_{max}, in differentiating between RIC and TP in brain metastasis patients. SUV_{peak}, due to its similar and in theory more flexible method of measurement, also shows promise. Further understanding of SUV_{peak} and how it compares with SUV_{max} in the context of brain metastases could lead to more effective follow-up treatment through earlier and improved clinical decision-making.

FUNDING

The authors declare no conflicts of interest. This study has received funding by the University of Groningen (Mandema stipend to A.H., Junior Scientific Masterclass grant B.D.).

REFERENCES

1. Achrol AS, Rennert RC, Anders C, Soffietti R, Ahluwalia MS, Nayak L, et al. Brain metastases. *Nat Rev Dis Primers* 2019; **5**: 5. doi: https://doi.org/10.1038/s41572-018-0055-y
2. Valiente M, Ahluwalia MS, Boire A, Brastianos PK, Goldberg SB, Lee EQ, et al. The evolving landscape of brain metastasis. *Trends Cancer* 2018; **4**: 176–96. doi: https://doi.org/10.1016/j.trecan.2018.01.003
3. Tabouret E, Chinot O, Metellus P, Tallet A, Viens P, Gonçalves A. Recent trends in epidemiology of brain metastases: an overview. *Anticancer Res* 2012; **32**: 4655–62.
4. Hardesty DA, Nakaji P. The current and future treatment of brain metastases. *Front Surg* 2016; **3**(Suppl 2): 1–7. doi: https://doi.org/10.3389/fsurg.2016.00030
5. Soffietti R, Abacioglu U, Baumert B, Combs SE, Kinhult S, Kros JM, et al. Diagnosis and treatment of brain metastases from solid tumors: guidelines from the European association of neuro-oncology (EANO. *Neuro Oncol* 2017; **19**: 162–74. doi: https://doi.org/10.1093/neuonc/now241
6. Franchino F, Rudà R, Soffietti R. Mechanisms and therapy for cancer metastasis to the brain. *Front Oncol* 2018; **8**: 1–28. doi: https://doi.org/10.3389/fonc.2018.00161
7. Lin NU, Lee EQ, Aoyama H, Barani IJ, Barboriak DP, Baumert BG, et al. Response assessment criteria for brain metastases: proposal from the RANO group. *Lancet Oncol* 2015; **16**: e270–8. doi: https://doi.org/10.1016/S1470-2045(15)70057-4
8. Chao ST, Ahluwalia MS, Barnett GH, Stevens GHJ, Murphy ES, Stockham AL, et al. Challenges with the diagnosis and treatment of cerebral radiation necrosis. *Int J Radiat Oncol Biol Phys* 2013; **87**: 449–57. doi: https://doi.org/10.1016/j.ijrobp.2013.05.015
9. Walker AJ, Ruzevick J, Malayeri AA, Rigamonti D, Lim M, Redmond KJ, et al. Postradiation imaging changes in the CNS: how can we differentiate between treatment effect and disease progression? *Future Oncol* 2014; **10**: 1277–97. doi: https://doi.org/10.2217/fon.13.271
10. Dooms GC, Hecht S, Brant-Zawadzki M, Berthiaume Y, Norman D, Newton TH. Brain radiation lesions: MR imaging. *Radiology* 1986; **158**: 149–55. doi: https://doi.org/10.1148/radiology.158.1.3940373
11. Delgado-López PD, Riñones-Mena E, Corrales-García EM. Treatment-Related changes in glioblastoma: a review on the controversies in response assessment criteria and the concepts of true progression, pseudoprogression, pseudoresponse and radionecrosis. *Clin Transl Oncol* 2018; **20**: 939–53. doi: https://doi.org/10.1007/s12094-017-1816-x
12. Thust SC, van den Bent MJ, Smits M. Pseudoprogression of brain tumors. *J Magn Reson Imaging* 2018; **48**: 571–89. doi: https://doi.org/10.1002/jmri.26171
13. Ellingson BM, Chung C, Pope WB, Boxerman JL, Kaufmann TJ. Pseudoprogression, radionecrosis, inflammation or true tumor progression? challenges associated with glioblastoma response assessment in an evolving therapeutic landscape. *J Neurooncol* 2017; **134**: 495–504. doi: https://doi.org/10.1007/s11060-017-2375-2
14. Sneed PK, Mendez J, Vemer-van den Hoek JGM, Seymour ZA, Ma L, Molinaro AM, et al. Adverse radiation effect after stereotactic radiosurgery for brain metastases: incidence, time course, and risk factors. *J Neurosurg* 2015; **123**: 373–86. doi: https://doi.org/10.3171/2014.10.JNS141610
15. Glaudemans AWJM, Enting RH, Heesters MAAM, Dierckx RAJO, van Rheenen RWJ, Walenkamp AME, et al. Value of 11C-methionine PET in imaging brain tumours and metastases. *Eur J Nucl Med Mol Imaging* 2013; **40**: 615–35. doi: https://doi.org/10.1007/s00259-012-2295-5
16. Terakawa Y, Tsuyuguchi N, Iwai Y, Yamanaka K, Higashiyama S, Takami T, et al. Diagnostic accuracy of 11C-methionine PET for differentiation of recurrent brain tumors from radiation necrosis after radiotherapy. *J Nucl Med* 2008; **49**: 694–9. doi: https://doi.org/10.2967/jnumed.107.048082
17. Grosu A-L, Astner ST, Riedel E, Nieder C, Wiedenmann N, Heinemann F, et al. An interindividual comparison of O-(2-[18F]fluoroethyl)-L-tyrosine (FET)- and L-[methyl-11C]methionine (MET)-PET in patients with brain gliomas and metastases. *Int J Radiat Oncol Biol Phys* 2011; **81**: 1049–58. doi: https://doi.org/10.1016/j.ijrobp.2010.07.002
18. Yomo S, Oguchi K. Prospective study of ^{11}C-methionine PET for distinguishing between recurrent brain metastases and radiation necrosis: limitations of diagnostic accuracy and long-term results of salvage treatment. *BMC Cancer* 2017; **17**: 713. doi: https://doi.org/10.1186/s12885-017-3702-x
19. Okamoto S, Shiga T, Hattori N, Kubo N, Takei T, Katoh N, et al. Semiquantitative analysis of C-11 methionine PET may distinguish brain tumor recurrence from radiation necrosis even in small lesions. *Ann Nucl Med* 2011; **25**: 213–20. doi: https://doi.org/10.1007/s12149-010-0450-2
20. Yamane T, Sakamoto S, Senda M. Clinical impact of (11)C-methionine PET on expected management of patients with brain neoplasm. *Eur J Nucl Med Mol Imaging* 2010; **37**: 685–90. doi: https://doi.org/10.1007/s00259-009-1302-y
21. Minamimoto R, Saginoya T, Kondo C, Tomura N, Ito K, Matsuo Y, et al. Differentiation of brain tumor recurrence from post-radiotherapy necrosis with 11C-methionine PET: visual assessment versus quantitative assessment. *PLoS One* 2015; **10**: e0132515. doi: https://doi.org/10.1371/journal.pone.0132515
22. Vander Borght T, Asenbaum S, Bartenstein P, Halldin C, Kapucu O, Van Laere K, et al. EANM procedure guidelines for brain tumour imaging using labelled amino acid analogues. *Eur J Nucl Med Mol Imaging* 2006; **33**: 1374–80. doi: https://doi.org/10.1007/s00259-006-0206-3
23. van Dijken B, Ankrah A, Stormezand G, et al. Prognostic value of 11C-methionine PET in patients with IDH wild-type glioma (Abstract. *J Nucl Med* 2019; **60**: 1501.

24. Galldiks N, Langen K-J, Albert NL, Chamberlain M, Soffietti R, Kim MM, et al. Pet imaging in patients with brain metastasis-report of the RANO/PET group. *Neuro Oncol* 2019; **21**: pp.: 585–95. doi: https://doi.org/10.1093/neuonc/noz003
25. Brahm CG, den Hollander MW, Enting RH, de Groot JC, Solouki AM, den Dunnen WFA, et al. Serial FLT PET imaging to discriminate between true progression and pseudoprogression in patients with newly diagnosed glioblastoma: a long-term follow-up study. *Eur J Nucl Med Mol Imaging* 2018; **45**: 2404–12. doi: https://doi.org/10.1007/s00259-018-4090-4
26. Brandsma D, Stalpers L, Taal W, Sminia P, van den Bent MJ. Clinical features, mechanisms, and management of pseudoprogression in malignant gliomas. *Lancet Oncol* 2008; **9**: 453–61. doi: https://doi.org/10.1016/S1470-2045(08)70125-6
27. Tsuyuguchi N, Sunada I, Iwai Y, Yamanaka K, Tanaka K, Takami T, et al. Methionine positron emission tomography of recurrent metastatic brain tumor and radiation necrosis after stereotactic radiosurgery: is a differential diagnosis possible? *J Neurosurg* 2003; **98**: 1056–64. doi: https://doi.org/10.3171/jns.2003.98.5.1056
28. Aide N, Lasnon C, Veit-Haibach P, Sera T, Sattler B, Boellaard R. EANM/EARL harmonization strategies in PET quantification: from daily practice to multicentre oncological studies. *Eur J Nucl Med Mol Imaging* 2017; **44**(Suppl 1): 17–31. doi: https://doi.org/10.1007/s00259-017-3740-2
29. Dankbaar JW, Snijders TJ, Robe PA, Seute T, Eppinga W, Hendrikse J, et al. The use of (18)F-FDG PET to differentiate progressive disease from treatment induced necrosis in high grade glioma. *J Neurooncol* 2015; **125**: 167–75. doi: https://doi.org/10.1007/s11060-015-1883-1
30. Sher A, Lacoeuille F, Fosse P, Vervueren L, Cahouet-Vannier A, Dabli D, et al. For avid glucose tumors, the SUV peak is the most reliable parameter for [(18)F]FDG-PET/CT quantification, regardless of acquisition time. *EJNMMI Res* 2016; **6**: 21. doi: https://doi.org/10.1186/s13550-016-0177-8
31. Ceccon G, Lohmann P, Stoffels G, et al. DynamicO-(2-18F-fluoroethyl)-L-tyrosine positron emission tomography differentiates brain metastasis recurrence from radiation injury after radiotherapy. *Neuro Oncol* 2016; **19**: 281–8.
32. Lizarraga KJ, Allen-Auerbach M, Czernin J, DeSalles AAF, Yong WH, Phelps ME, et al. ^{18}F-FDOPA PET for differentiating recurrent or progressive brain metastatic tumors from late or delayed radiation injury after radiation treatment. *J Nucl Med* 2014; **55**: 30–6. doi: https://doi.org/10.2967/jnumed.113.121418
33. Minniti G, Clarke E, Lanzetta G, Osti MF, Trasimeni G, Bozzao A, et al. Stereotactic radiosurgery for brain metastases: analysis of outcome and risk of brain radionecrosis. *Radiat Oncol* 2011; **6**: 48. doi: https://doi.org/10.1186/1748-717X-6-48